Journal of Hydroscience and Hydraulic Engineering
Vol. 30, No.2 November, 2012, 27-38

ANALYSIS OF A DEEP-SEATED LANDSLIDE IN SHAOLIN VILLAGE, KAOHSIUNG COUNTY, TAIWAN

By

Daizo Tsutsumi

Disaster Prevention Research Institute, Kyoto University, Okuhida-Onsengo Takayama, Gifu, Japan

Masaharu Fujita

Disaster Prevention Research Institute, Kyoto University, Fushimi Kyoto, Kyoto, Japan

Kuniaki Miyamoto

Graduate School of Life and Environmental Sciences, Tsukuba University, Tsukuba, Ibaraki, Japan

Fujitoshi Imaizumi

Graduate School of Life and Environmental Sciences, Tsukuba University, Ikawa, Shizuoka, Japan

Masamitsu Fujimoto

College of Science and Engineering, Ritsumeikan University, Kusatsu, Shiga, Japan

Hiroshi Kokuryo

Nippon Steel & Sumikin Metal Products Co.,Ltd., Koto-ku, Tokyo, Japan

and

Hiroaki Izumiyama

Yachiyo Engineering Co., Ltd., Shinjuku-ku, Tokyo, Japan

SYNOPSIS

In August 2009, Typhoon Morakot struck Taiwan, producing an extraordinary amount of rainfall. The heavy rainfall caused a large number of floods and sediment-related disasters across the island. In Shaolin Village, Kaohsiung County, a huge landslide, about 1,200 m long, 500 m wide, and 80 m deep, occurred around 6:00 on August 9th, destroying the village and killing more than 500 people. After the landslide, we visited the landslide site and investigated the landslide scour to collect information about factors affecting landslide occurrence such as exposed bedrock and soil layer conditions. Geographic information system (GIS) analysis using digital elevation model data

was also conducted to determine the sliding domain. On the basis of the site investigation and GIS analysis, rainwater infiltration and slope stability analyses were conducted. The simulated landslide occurred at the lower part of the slope, in contrast to the actual landslide. Although the exact process of the huge landslide in Shaolin Village is unknown, a multi-phase collapse was a possibility and the simulated landslide may represent the first step in this process.

INTRODUCTION

Typhoon Morakot struck Taiwan from August 6th to August 10th 2009, bringing huge amounts of rain to the entire island. Precipitation was especially heavy in the central and southern parts of the island, where over 3,000 mm of precipitation was recorded. Such heavy rainfall caused flooding and sediment-related disasters resulting in many deaths. The most severe disaster was the deep-seated landslide occurred in Shaolin Village, Kaohsiung County, which destroyed the whole village at the foot of the slope and killed more than 500 people. We visited the site after the disaster and investigated the landslide scar to clarify the mechanisms behind such a deep-seated landslide. Geographic information system (GIS), rainwater infiltration, and slope stability analyses were conducted. From the results of the analyses the exact shape and size of the landslide, the relationship between rainfall and landslide occurrence, the underground water conditions within the slope layers at the time of landslide occurrence were revealed. Whether a single process or multi-phase processes occurred during the landslide is a matter to be discussed in this paper.

OUTLINE OF THE DISASTER

Shaolin Village used to sit at the foot of a slope on the south side of the Chishan River. According to Shieh et al. (1), more than 1,500 mm of rain fell in the Shaolin area the night before the landslide (8 August), and several warning and evacuation notices were issued. However, roads and bridges for the evacuation had already been destroyed by debris flows, and people in the main part of Shaolin Village were isolated. More than 500 people gathered at an elementary school, which was considered a safe shelter. Around 6:00 on the morning of the 9th of August, part of the 2.5 km slope above the village collapsed. The sliding mass destroyed the whole village and completely destroyed the school, killing all of the people sheltering inside (Fig. 1). The sliding mass continued flowing to the Chishan River, where it formed a 50 m high landslide dam, which collapsed 40 minutes later.

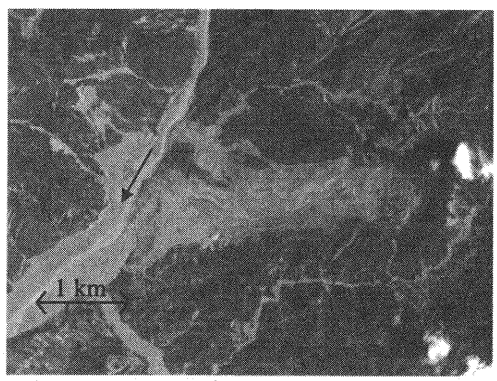

Fig. 1 Aerial photo of the deep seated landslide in Shaolin village, Kaohsiung County, Taiwan. (provided by National Cheng Kung University)

PROPERTIES RELATING TO THE LANDSLIDE OCCURRENCE

Rainfall

Figure 2 shows the rainfall recorded at a station close to Shaolin Village from April to August 2009. Before the rainstorm in early August, several rainfall events were observed with total precipitation amounting to 1,000 mm. Due to the influence of Typhoon Morakot, precipitation increased suddenly and heavy rainfalls continued from 6 to 10 August. During the afternoon of 8 August, very high rainfall intensity (110 mm/h) was recorded, with rainfall of 20 mm/h intensity recorded for almost half of the duration of rainfall (Fig. 3). This long-lasting and intense rainfall was caused by the slow-moving typhoon, which lingered over the island of Taiwan for a long time. Clearly, this extraordinary amount of rainfall infiltrated into the deep layer of the slope, making the slope instable, which ultimately caused such deep-seated landslide.

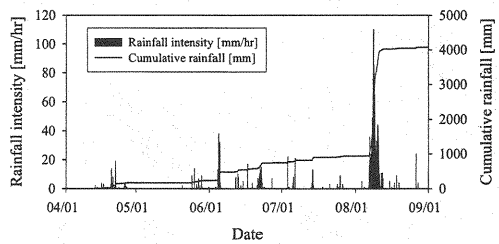

Fig. 2 Rainfall record at a observation station close to Shaolin village (from 2009/ 4/1 to 8/31)

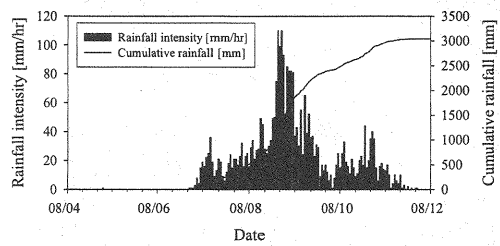

Fig. 3 Rainfall induced by Typhoon Morakot (from 2009/8/4 to 12)

Topographic change

Figure 4 shows the topographic changes around the deep-seated landslide and Shaolin Village before and after the landslide on 9 August, drawn from digital elevation model (DEM) data. Comparison of the upper and middle figures reveals considerable changes in slope topography at the center of the figures. The relatively smooth slope surface before August 8th became a rough surface with a striped appearance after the landslide (middle to upper right of the figures). During our site investigation after the disaster, we found that discontinuous bedrock was exposed to reveal a stripe-shaped geomorphology along the slope direction; this is shown in the DEM data as the gully topography after the disaster. The area with the large geomorphic change seems to have been the main part of the landslide. The comparison also reveals that a valley became relatively flat due to sedimentation at a lower part of the slope. These changes are more clearly illustrated in the bottom panel in Fig. 4, which shows the difference in elevation level after the disaster. As shown in this figure, changes in elevation occurred not only in the main part of the landslide

but also in surrounding areas, where many other slope failures occurred.

To investigate topographic changes in more detail, lines A-A', B-B', C-C', and D-D' were drawn on the slope (Fig. 5), and longitudinal and cross sections of the slope along each line were obtained from DEM data. The results are shown in Figs. 6 and 7. The longitudinal and cross sections (Figs. 6 and 7) clearly show erosion in the upper (1 km) part of the slope (B-B'), accumulation at the lowermost (1 km) part of the slope (D-D'), and an unchanged area (C-C') between the eroded and accumulated parts. During site observation, we found that bedrock was exposed around the unchanged part (C-C'), as shown in Fig. 8. This evidence suggests that no erosion and accumulation occurred in the unchanged area. Therefore, this unchanged area divides the eroded upper part and the accumulated lower part. We can deduce that only the upper area collapsed and the sliding mass flowed down across the unchanged area to Shaolin Village and the Chishan River. A portion of the sliding mass accumulated at the lower part. Based on a comparison of elevation before and after the landslide (Fig. 4), we estimated that the landslide had a maximum depth of 84 m, average depth of 50 m, length of 1,100 m, and maximum width of 500 m. We also found evidence of landslide dam formation on the Chishan River bank as shown in Figs. 4 and 6, which was previously reported by Hara et al. (2).

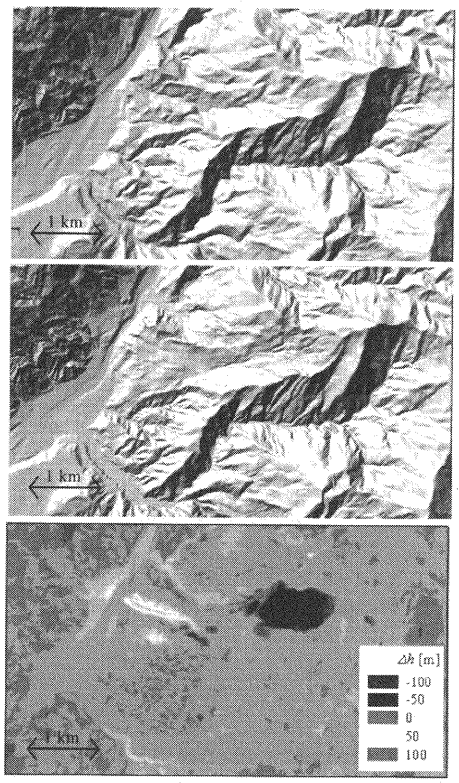

Fig. 4 Topographical change of the slope in Shaolin village produced from DEM data (top: before the landslide, middle: after the landslide, bottom: difference

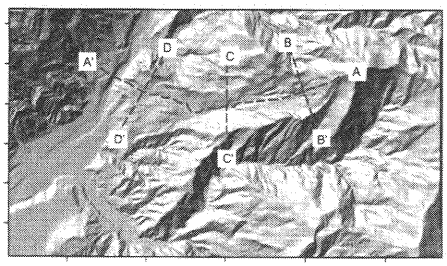

Fig. 5 Longitudinal and lateral lines on the slope.

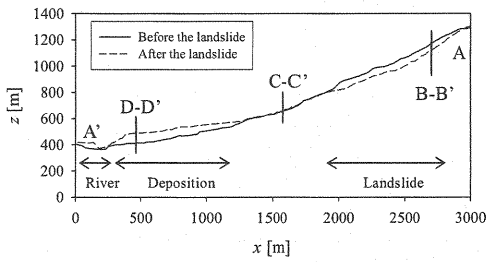

Fig. 6 Topographical change of longitudinal section (A-A') before and after the landslide.

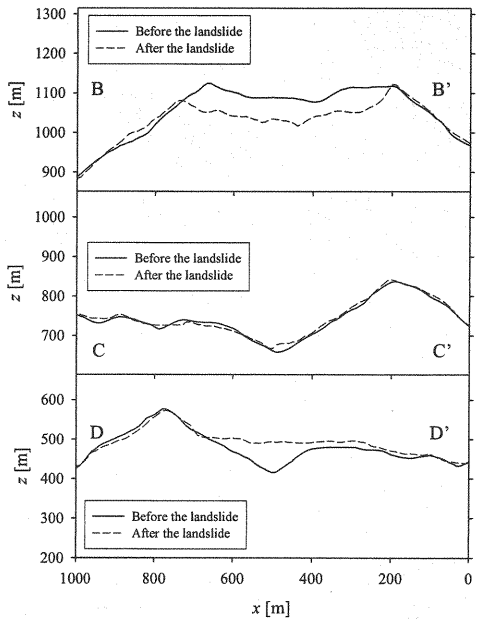

Fig. 7 Topographical change of cross sections (B-B', C-C', D-D') before and after the landslide.

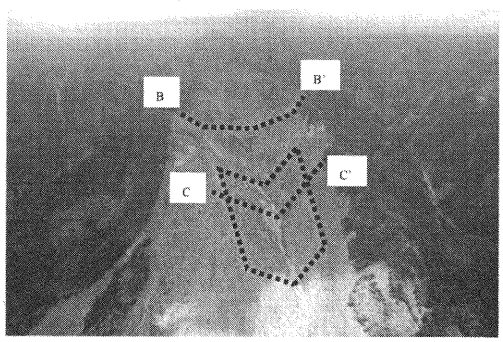

Fig. 8 Bedrock exposure at the middle slope, where the topography didn't change (provided by National Cheng Kung University).

Hydraulic properties of the soil layer

Geological investigation at the slope revealed layers of weathered sandstone and shale, underlain by sandstone bedrock. Some mudstone layers also appeared at the lower end of the slope. Because the accumulated sediment and remaining sliding mass consisted of clayey sediment and large quantities of sandstone debris, the slope layer before the landslide likely consisted of a mixture of weathered soil and sandstone rocky layers. Soil samples were collected from the remaining sliding mass (bottom and middle layers) and surface layer surrounding the landslide at the site. Approximate locations of soil sampling are indicated in Fig.9. For the soil samples, pF tests were conducted in a laboratory. The measured water retention curves for the sampled soils are shown in Fig. 10. A sample collected from

the bottom layer just above the bedrock appeared to be weathered sandstone. The soil from the middle and bottom layers had relatively low volumetric water content compared to common forest soils. The hydraulic conductivity of each soil sample was also measured. The measured saturated hydraulic conductivities were 2.5×10^{-2} cm/s at the surface, 1.6×10^{-3} cm/s in the middle layer, and 8.5×10^{-4} cm/s at the bottom layer. The measured saturated hydraulic conductivity results suggest that deeper soils had lower conductivity. However, even soil at the bottom layer had relatively high conductivity. Such hydraulic properties suggest that the entire slope layer had relatively high permeability, and that pore water pressure tended to increase easily. According to the site investigation, the collapsed slope consisted of a heterogeneous composition, with large rocks and varied soil formation, so preferential pathways could have formed through cracks or fractures in the rocks and rainwater might have run more quickly to deeper layer than ordinal soil layer.

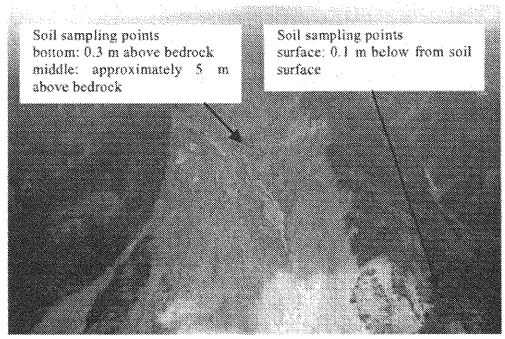

Fig. 9 Locations of soil sampling (bottom and middle layer at center of landslide scar, surface at the edge of scar)

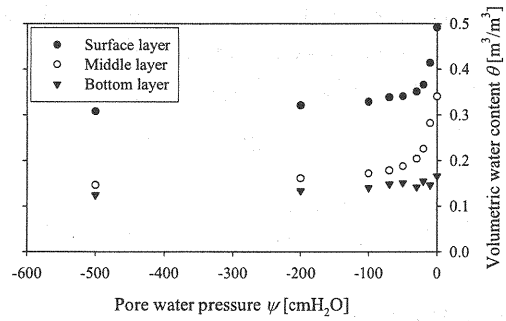

Fig. 10 Measured water retention curves for the sampled soils

Table 1 Fitting parameters for the soil hydraulic properties used in the rainwater infiltration analysis

Layer	K_s	θ_s	θ_r	ψ_m	σ
	cm/s	m^3/m^3	m^3/m^3	mH_20	-
Lower	0.005	0.34	0.15	-2.0	2.0
Upper	0.01	0.49	0.31	-0.5	1.6

RAINWATER INFILTRATION ANALYSIS

Method of analysis

A rainwater infiltration analysis was conducted, using the rainfall data, topographic data, and soil hydraulic properties described in the previous section. In general, three-dimensional analysis is preferable to clarify actual water infiltration. However, the objective slope was too extensive for practical three-dimensional simulation. The cross-section at the upper slope, where the landslide originated (B-B'), revealed a relatively flat surface and bedrock topography. Therefore, a two-dimensional analysis along the center of the slope was used to reduce the calculation load. In the analysis, the two-dimensional Richards' equation was solved by means of the finite element method. Tsutsumi and Fujita (3) described this method in detail. The finite elements were divided into 10 m constant intervals for slope direction and a maximum of 1.5 m intervals for depth direction.

The lognormal model by Kosugi (4) was employed to express the water retention curve. Table 1 lists the fitting parameters used in the analysis. The slope was divided into upper and lower layers, and different soil hydraulic properties were employed for each layer according to the results of the pF test shown in Fig. 10. As noted above, the slope had a heterogeneous composition, with large rocks and varied soil formation, so preferential pathways could have formed through cracks or fractures in the rocks. In the present simulation, these heterogeneous conditions could not be considered precisely. To reflect fast infiltration through preferential pathways, we assigned hydraulic conductivities greater than measured values to each layer.

For the upslope end and bottom of the soil layer, a no-flux boundary condition was imposed. For the downslope end, a seepage face boundary condition was imposed. The observed rainfall was applied to the soil surface. To prepare the initial condition of soil moisture, 240 mm total rainfall over a 24 hr duration was applied to the surface, which was then left to drain freely for 36 hrs.

The slope stability analysis was conducted simultaneously with the infiltration analysis. A simplified Janbu method was employed for the slope stability analysis because such a method can be applied to any shape of slip surface. In the simplified Janbu method, the soil layer was divided into vertical slices, and the balance of stresses and slip condition within each slice was examined. The factor of safety F_s calculated by the simplified Janbu method is expressed as

$$F_s = \frac{\sum \left[\{ c_i' l_i \cos a_i + (W_i - u_i l_i \cos a_i) \tan \phi_i' \} / m_a \right]}{\sum W_i \tan a_i} \tag{1}$$

$$m_a = \cos^2 a_i \left(1 + \tan a_i \tan \phi_i' / F_s\right) \tag{2}$$

where subscript i = the number of vertical slices in the soil layer, c_i' and ϕ_i' = cohesion and internal friction angle of the soil, respectively, W_i = weight of the slice, a_i and l_i = angle and length of slip surface within the slice, respectively, and u_i = the water pressure affected on the slip surface.

The dynamic programming (DP) method described by Kubota and Nakamura (5) was used to identify the slip surface that provides the minimum safety factor. The spatial distribution of the pore water pressure, which was calculated by means of the rainwater infiltration analysis, was used in the slope stability analysis as input data. An assumed internal friction angle ϕ' and cohesion c' of the soil were employed, so the model approximates the actual landslide size and timing accurately.

Results of analysis

Figure 11 presents simulated distributions of pore water pressure in the longitudinal section of the objective sloped soil domain at the initial time (a: 3:00, 4 August 2009), just before the rainfall started (b: 18:00, 8 August 2009), and at the time of the simulated landslide (c: 1:00, 8 August 2009). The assumed initial moisture condition in Fig. 11a shows a very homogeneous distribution of pore water pressure. After 240 mm total rainfall application and free drainage for 36 hr, pore water pressure was distributed as shown in Fig. 11b. Figure 11b shows naturally distributed pore water pressure in contrast to Fig. 11a. However, because the practical total amount of water within the sloped soil domain is unknown, it is impossible to determine whether this initial moisture condition reproduced a realistic condition. The simulated rainwater infiltration applied the recorded rainfall and calculated slope stability, and safety factor F_s decreased below 1.0 at 16:00 on 8 August (Fig. 12). In Figure 11c, the underground water table is evenly developed from the downslope end toward the upslope end. This highly developed underground water table might be the result of vertical infiltration being superior to lateral infiltration under the conditions of a gentle slope gradient and a very deep slope layer. The simulated landslide occurred in the lower part of the slope (Fig. 11c), in contrast to the actual landslide (Fig. 6). According to a previous study conducted by Tsutsumi et al. (6), it was empirically and experimentally demonstrated that some slopes collapse in a multi-phase manner. Although the exact process of the huge landslide in Shaolin Village is unknown, multi-phase collapse is a possibility and the simulated landslide may represent the first step in this process. To elucidate the landslide process in detail, a simulation method that can consider multi-phase collapse must be developed. The simulated time of landslide occurrence (16:00, 8 August) is also much earlier than the actual time (6:20, 9 August). There are several possible reasons for this disagreement, such as simplification of the soil domain and assumed soil properties. The initial moisture condition is one of the most important factors affecting simulation. To assess the effect of initial moisture condition on the timing of landslide occurrence, calculated changes in the total amount of water retained in the sloped soil domain is shown with applied rainfall in Fig. 13. The figure reveals that the total amount of water continued to increase from after rainfall began (18:00, 6 August) until rainfall peaked (18:00, 8 August), although rainfall fluctuated. After rainfall peaked, the total amount of water stopped rising. After almost the entire soil domain was saturated, the applied rainwater and drainage water may have become balanced. The difference in total water retained in the soil domain was 1390 m^3, which is only 6% of the total amount of water in the soil domain. This finding implies that the time of landslide occurrence (which is similar to the time of saturation of the soil domain) was greatly affected by the initial moisture condition. Therefore, if the retained soil water had been slightly reduced at the initial stage, the simulated time of landslide occurrence would have been delayed drastically.

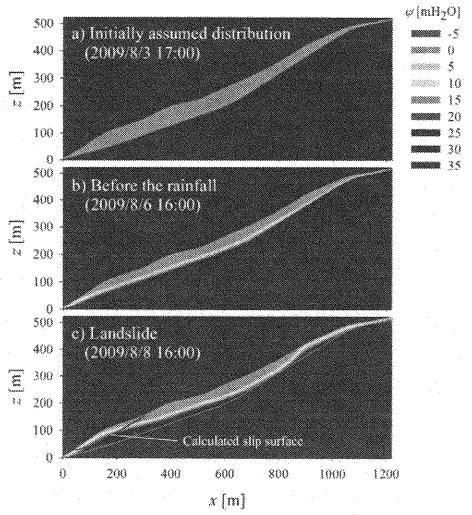

Fig. 11 Results of the simulation: a) assumed initial condition, b) at just before the rain starts, and c) at the landslide occurrence (red line indicates the simulated slip surface).

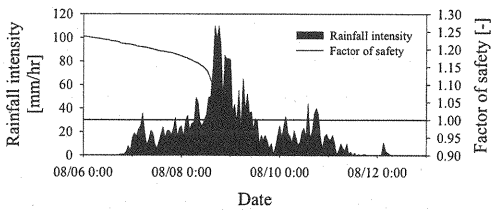

Fig. 12 Simulated factor of safety F_s (red line) with applied rainfall (blue bars).

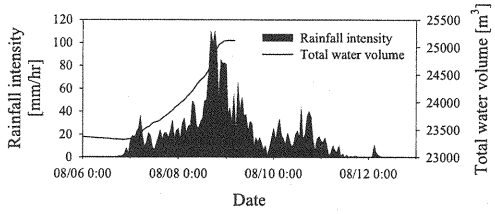

Fig. 13 Simulated change of total retention water in the sloped domain.

CONCLUSIONS

In the present research, post-landslide site investigation, topographic analysis by GIS, and rainwater infiltration and slope stability analyses were conducted to investigate the mechanism of the deep-seated landslide that devastated

Shaolin Village, Taiwan. The results suggest that a huge amount of rainfall infiltrated the deep soil layer, leading to a highly developed water table, especially around the downslope end. These factors destabilized the slope, which eventually collapsed, and the results suggest that the slope may have collapsed in a multi-phase manner.

However, this simulation approach posed some limitations that should be addressed. First, it is important to assume an appropriate initial moisture condition in the calculation soil domain because this condition can have a considerable effect on the timing of simulated landslide occurrence. Secondly, the heterogeneous mix of soil and large rocks and the preferential pathways through bedrock fractures or soil pipes were neglected in the simulation. Only the soil hydraulic conductivity was increased from the measured values to reflect rapid water infiltration through preferential pathways, which did not express the actual water transportation in the slope. Thirdly, the present method of slope stability analysis cannot simulate multi-phase slope failures. Rainwater infiltration and slope stability analyses should be continued after the occurrence of the first landslide, removing the sliding soil mass and modifying the calculation soil domain to simulate a multi-phase landslide.

Because of such problems and the simplification of the analysis, the simulated results did not accurately reproduce the actual landslide. However, this challenge of simulating an extraordinarily huge landslide highlights the unique problems of large-scale landslide modeling, and can benefit future efforts to improve landslide modeling and disaster mitigation research.

REFERENCES

1. Shieh C. L., Tsai, Y. J., Lai, W. C., Chen, Y. S., Chen, K. T. and Chiu, C. L.: Disasters caused by Typhoon Morakot in Taiwan and the renovation strategy, Proceedings of the International Symposium on Water and Sediment Disasters in East Asia, pp. 36-44, 2010.
2. Hara, Y., Uchida, T., Yoshino, H., Miyamoto, K., Gonda, Y. and Imaizumi, F.: Erosion of the landslide dam by overtopping flow at Shaolin Village, Taiwan, during Typhoon Morakot, proceedings of Japan Society of Erosion Control Engineering, pp. 90-91, 2010 (in Japanese, with title tentatively translated by the author).
3. Tsutsumi, D. and Fujita, M.: Relative importance of slope material properties and timing of rainfall for the occurrence of landslides, International Journal of Erosion Control Engineering, 1 (2), pp. 79-89, 2008.
4. Kosugi, K.: Lognormal distribution model for unsaturated soil hydraulic properties, Water Resources Research, 32, pp. 2697-2703, 1996.
5. Kubota, T. and Nakamura, H.: Landslide susceptibility estimation by critical slip surface analysis combined with reliable analysis, Journal of the Japan Landslide Society, Vol. 27 (4), pp. 18-25, 1991 (in Japanese).
6. Tsutsumi, D. and Fujita, M.: Effect of slope material properties on the timing, size and processes of landslides, Journal of Hydroscience and Hydraulic Engineering, 27 (1), JSCE, pp. 105-119, 2009.

APPENDIX – NOTATION

The following symbols are used in this paper:

a_i = angle of the slip surface within the i^{th} slice;

c' = cohesion;

c_i' = cohesion of the soil at the i^{th} vertical slice;

F_s = factor of safety;

i = number of vertical slices in the soil layer;

K_s = saturated hydraulic conductivity;

l_i = length of the slip surface within the i^{th} slice;

u_i = water pressure affected on the slip surface at the i^{th} slice;

W_i = weight of the i^{th} slice;

ϕ' = internal friction angle;

ϕ_i' = internal friction angle of the soil at the i^{th} vertical slice;

θ_r = residual volumetric water content;

θ_s = saturated volumetric water content;

σ = a dimensionless parameter related to the width of the pore-size distribution in the lognormal model;

ψ_m = pressure potential corresponding to the median soil pore radius in the lognormal model.

(Received Aug, 02, 2011 ; revised Jun, 13, 2012)